電気化学会関西支部　第 51 回電気化学講習会
電気化学の基礎と新しいアプローチ

２．分極曲線の考え方〜腐食，ナトリウムイオン電池，
電気二重層キャパシタ，燃料電池〜　（その２）

（産業技術総合研究所）倉谷健太郎
（京都大学）深見一弘
（大阪大学）土谷博昭
（鳥取大学）薄井洋行
（大阪公立大学）知久昌信
（産業技術総合研究所）山崎眞一

Electrochemical Polarization Part 2: Electrochemical Devices

Hiroyuki USUI,[a] Masanobu CHIKU,[b] Shin-ichi YAMAZAKI,[c] Kentaro KURATANI,[c,*] Kazuhiro FUKAMI,[d] and Hiroaki TSUCHIYA[e]

[a] *Graduate School of Engineering, Tottori University, 4-101 Koyama-cho Minami, Tottori 680-8552, Japan*
[b] *Graduate School of Engineering, Osaka Metropolitan University, 1-1 Gakuen-cho, Naka-ku, Sakai, Osaka 599-8531, Japan*
[c] *Research Institute of Electrochemical Energy, National Institute of Advanced Industrial Science and Technology (AIST), 1-8-31 Midorigaoka, Ikeda, Osaka 563-8577, Japan*
[d] *Department of Materials Science and Engineering, Kyoto University, 36-1 Yoshida-Hommachi, Sakyo-ku, Kyoto 606-8501, Japan*
[e] *Graduate School of Engineering, Osaka University, 2-1 Yamadaoka, Suita, Osaka 565-0871, Japan*

* *Corresponding author: k-kuratani@aist.go.jp*

Electrochemical Polarization Part 2: Electrochemical Devices ~Sodium-ion battery~

Hiroyuki USUI,[a] Masanobu CHIKU,[b] Shin-ichi YAMAZAKI,[c] Kentaro KURATANI,[c] Kazuhiro FUKAMI,[d] Hiroaki TSUCHIYA,[e]

[a] Graduate School of Engineering, Tottori University, 4-101, Koyama-cho minami, Tottori, 680-8552, Japan

[b] Graduate School of Engineering, Osaka Metropolitan University, 1-1, Gakuen-cho, Naka-ku, Sakai, Osaka, 599-8531, Japan
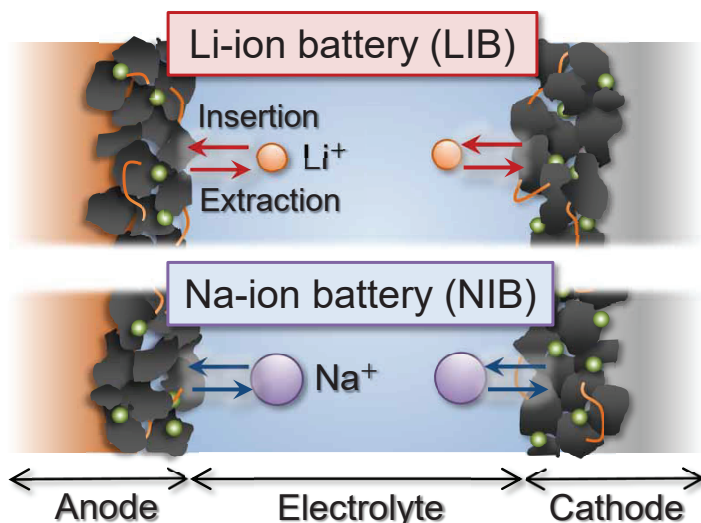
[c] Research Institute of Electrochemical Energy, National Institute of Advanced Industrial Science and Technology (AIST), 1-8-31, Midorigaoka, Ikeda, Osaka, 563-8577, Japan

[d] Department of Materials Science and Engineering, Kyoto University, 36-1, Yoshida-Hommachi, Sakyo-ku, Kyoto, 606-8501, Japan
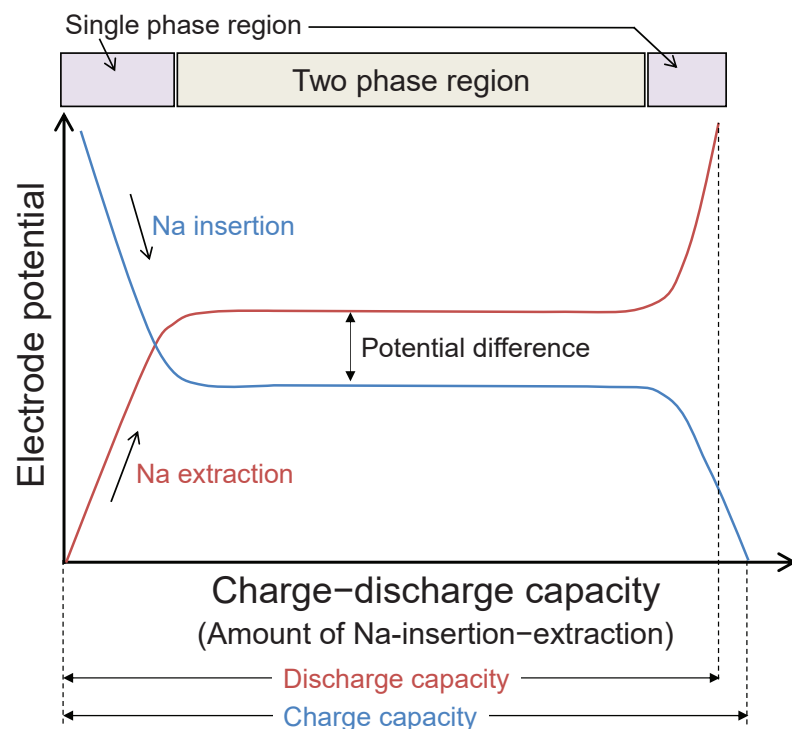
[e] Graduate School of Engineering, Osaka University, 2-1, Yamadaoka, Suita, Osaka, 565-0871, Japan

---

Charge−discharge curves of Na-ion battery

Na-ion battery:
One of the most attractive energy storage devices

Li-ion battery (LIB)
Insertion
Li⁺
Extraction

Na-ion battery (NIB)
Na⁺

Anode   Electrolyte   Cathode

Typical charge−discharge curves of anodes

Single phase region — Two phase region

Electrode potential

Na insertion

Potential difference

Na extraction

Charge−discharge capacity
(Amount of Na-insertion−extraction)

Discharge capacity
Charge capacity

63

Background of Na-ion battery

Li-ion battery (LIB)

Insertion → Li+ ← Extraction

Active material

Na-ion battery (NIB)

Na+

Anode — Electrolyte — Cathode

◎ **Advantages of Na resources**

Low-cost and ubiquitous

△ **Required material research**

M. Shimizu, H. Usui, K. Fujiwara, K. Yamane, H. Sakaguchi, *J. Alloys Compd.*, **640** (2015) 440.

Charge−discharge curves of Si

Potential / V vs. Li$^+$/Li, Na$^+$/Na

Li-ion battery

Na-ion battery

Capacity / mA h g^{-1}

Na$^+$ ✕ Bulk Si ⟵ Li$^+$

Material research is needed for NIB.

Three kinds of Na-storage reactions as anodes

Insertion type

	Resistivity / Ω cm	Density / g cm^{-3}	Sodiation composition	Theoretical capacity / mA h g^{-1}	Volume expansion ($V_{sodiated}/V_0$)	Cost / \$ kg^{-1}
Hard carbon	10^{-4}	< 1.5	Na$_{0.16}$C	*ca.* 350	*ca.* 110%	220
Rutile TiO$_2$	10^{13}	4.23	NaTiO$_2$	335	136%	10
CeO$_2$	10^9	7.22	NaCeO$_2$	156	153%	5

Alloying type

P	1.5×10^0	2.69	Na$_3$P	2596	490%	43
Sn	1.1×10^{-5}	7.37	Na$_{15}$Sn$_4$	847	520%	22
Si	10^5	2.33	Na$_{0.76}$Si	725	220%	2.1
Sb	3.9×10^{-5}	6.70	Na$_3$Sb	660	390%	11
Bi	1.1×10^{-5}	9.78	Na$_3$Bi	385	350%	10

Conversion type

Fe$_2$O$_3$	10^5	5.24	2Fe + 3Na$_2$O	1007	315%	0.2

Alloying-type anode materials

Hard carbon

  Good cyclability

  Moderate capacity

  （Typically 300−350 mA h g^{-1}）

P, Sn, and Sb

  High theoretical capacity

  High electronic conductivity
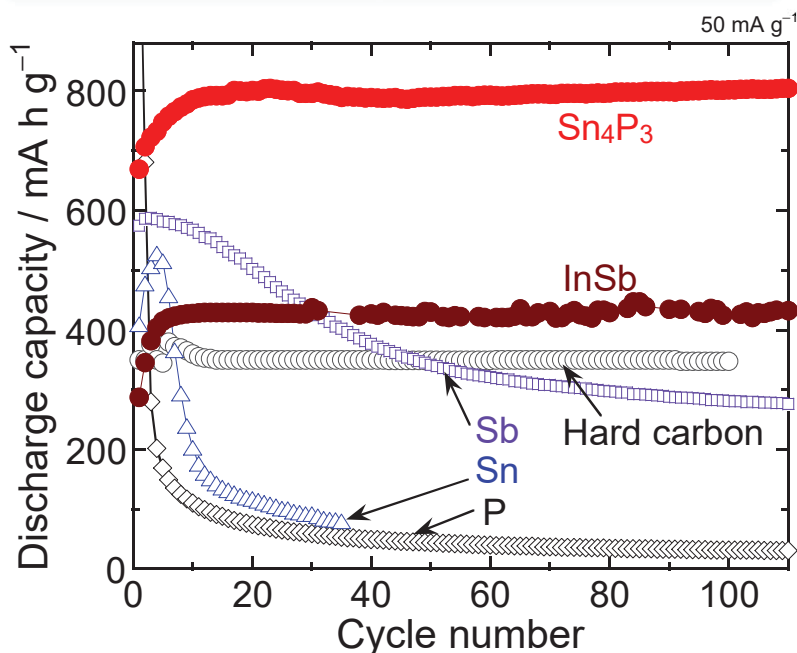
  Large volume changes during cycle

  Electrode disintegration

    ⮱ Rapid capacity decay

Improvement by formation of compound (Sn$_4$P$_3$) or alloy (InSb)

H. Usui, Y. Domi, K. Fujiwara, M. Shimizu, T. Yamamoto, T. Nohira, R. Hagiwara, H. Sakaguchi, *ACS Energy Lett.*, **2** (2017) 1139.

H. Usui, Y. Domi, N. Takada, H. Sakaguchi, *Cryst. Growth Des.*, **21** (2021) 218.

50 mA g^{-1}

Bismuth (Bi) as NIB anode material

Hard carbon

  Good cyclability

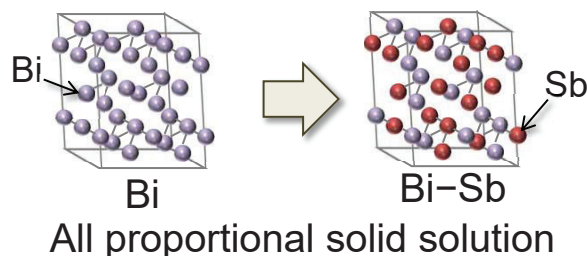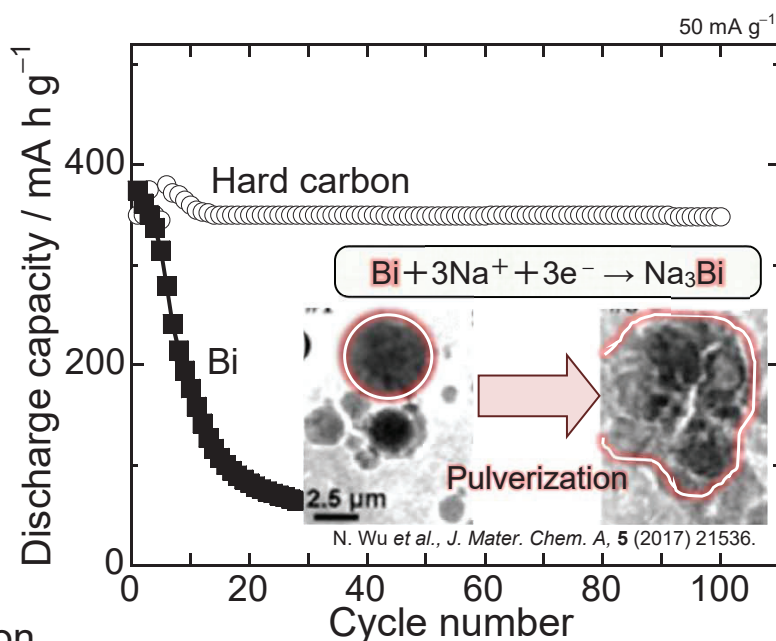 Moderate capacity

  （Typically 300−350 mA h g^{-1}）

Bismuth（Bi）

  High electronic conductivity

  Large volume changes （350%）

  Electrode disintegration by pulverization

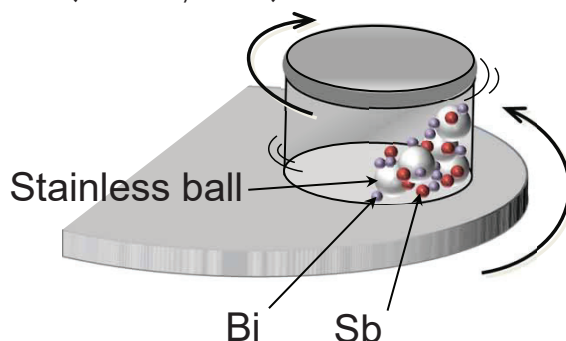Improving mechanical property by solid solution formation (Bi−Sb)

50 mA g^{-1}

$$Bi + 3Na^+ + 3e^- \rightarrow Na_3Bi$$

Pulverization

2.5 μm

N. Wu *et al.*, *J. Mater. Chem. A*, **5** (2017) 21536.

Bi → Bi−Sb

All proportional solid solution

64

Preparation of Bi−Sb solid solution

Active material preparation

Mechanical alloying method

Bi：Sb ratio	2:8, 5:5, 8:2
Duration time	4 h
Rotation speed	380 rpm
Ball and pod	Stainless steel
Ball : Bi−Sb ratio	30：1（weight）

Planetary ball milling machine
（Fritch, P-6）

Stainless ball

Bi   Sb

Film electrode preparation

Ratio   Bi−Sb / Acetylene black / Thickener / Binder
70% /   15%   /   10%   /   5%（in weight ratio）

Substrate   Al foil（18 μm）

Thickness   10 μm

Loading   1.5 mg cm^{-2}

Thickener: Carboxymethyl cellulose
Binder   : Styrene-butadiene rubber

Evaluation of Bi−Sb solid solution electrodes
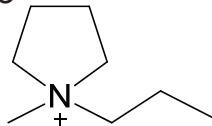
Charge−discharge test

Working electrode : Bi−Sb

Counter electrode   : Na

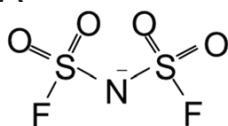Electrolyte : 1 M NaFSA/Py13-FSA

Py13   FSA

N-methyl-N-propylpyrrolidinium   bis(fluorosulfonyl)amide

Potential range : 0.005−2.0 V vs. Na$^+$/Na

Current density : 50 mA g^{-1}（0.09−012C）

10−1500 mA g^{-1}

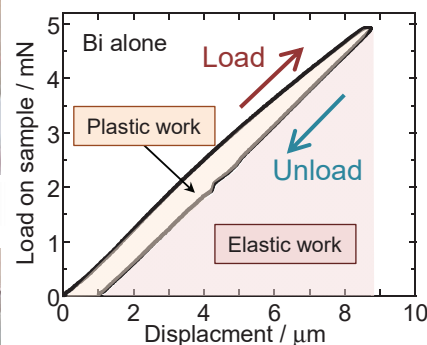Temperature : 30 $^{\circ}$C
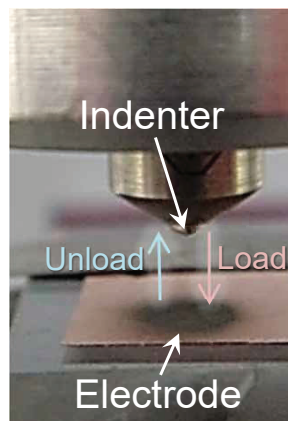
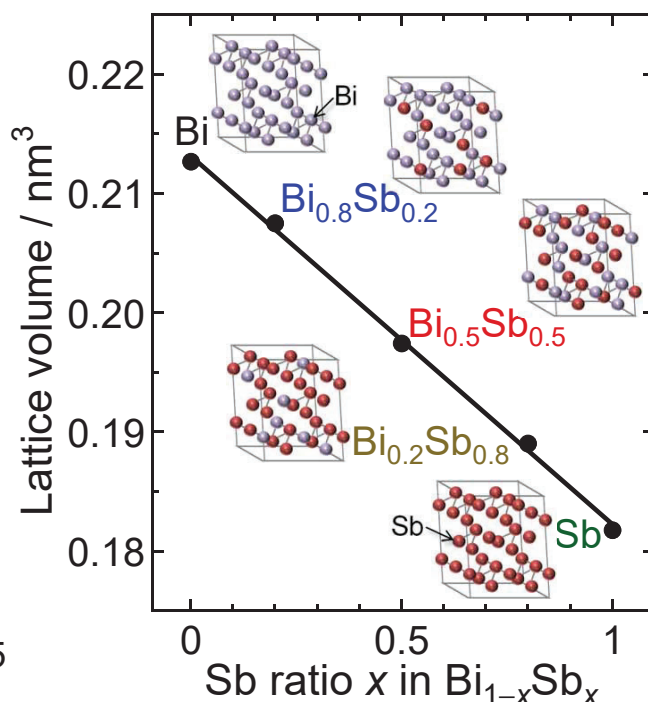2032-tyep coin cell

Characterization

X-ray diffraction（XRD）

X-ray fluorescent analysis（XRF）

Scanning electron microscope（SEM）

Cycling voltammetry（CV）

Nanoindentation test

Indenter

Unload   Load

Electrode

Bi alone

Load

Plastic work

Unload

Elastic work

65

Confirmation of Bi−Sb solid solution formation

- ● Bi, Bi–Sb, Sb
- ▽ Cu (Internal standard)

ICSD:00-005-0560 (Sb)
ICSD:01-081-3946 (Bi$_{0.5}$Sb$_{0.5}$)
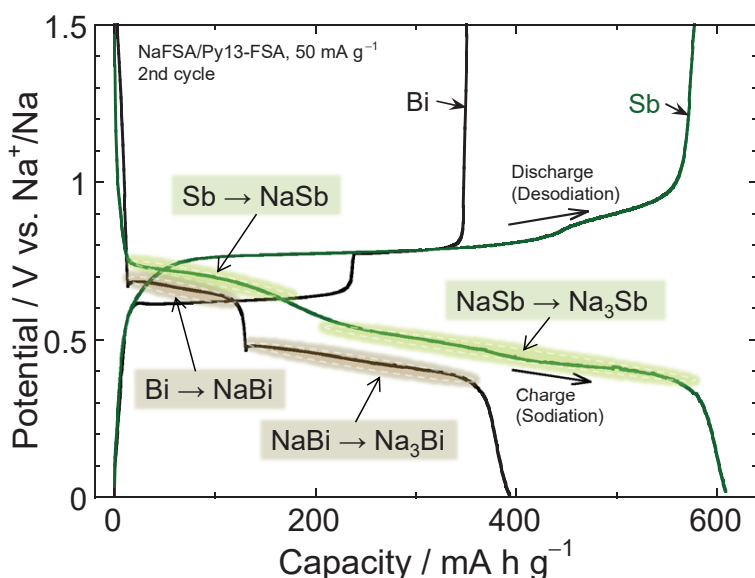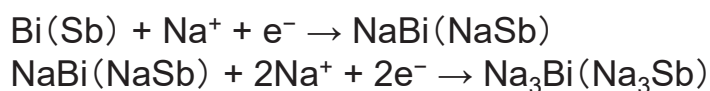ICSD:01-085-1330 (Bi)

Lattice volume was linearly reduced with increasing Sb ratio, demonstrating formation of Bi−Sb solid solutions.
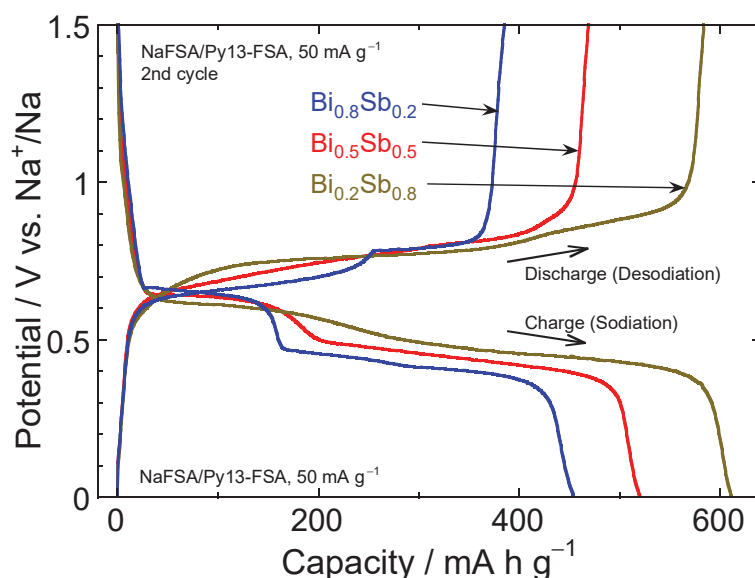
Charge−discharge curves of Bi−Sb electrodes

Bi electrode and Sb electrode

Bi−Sb electrodes

Two-step Na-storage reactions of Bi and Sb

Unclear potential plateaus of Bi$_{0.5}$Sb$_{0.5}$ and Bi$_{0.2}$Sb$_{0.8}$ electrodes

$$Bi(Sb) + Na^+ + e^- \rightarrow NaBi(NaSb)$$
$$NaBi(NaSb) + 2Na^+ + 2e^- \rightarrow Na_3Bi(Na_3Sb)$$

H. Usui, Y. Domi, Y. Itoda, H. Sakaguchi, *Energy & Fuels*, **35** (2021) 18833.

Charge−discharge curves of $Bi_{0.2}Sb_{0.8}$ at low *C*-rates

50 → 10 mA g⁻¹

Bi_{0.2}Sb_{0.8} electrode

Na(Bi,Sb)→(Bi,Sb)

Na_3(Bi,Sb)→Na(Bi,Sb)

Current density

50 mA g⁻¹
40
30
20
10

(Bi,Sb)→Na(Bi,Sb)

Na(Bi,Sb)→Na_3(Bi,Sb)

Theoretical capacity:
570 mA h g⁻¹ ($Bi_{0.2}Sb_{0.8}$)

Current density / mA g⁻¹	Charge capacity / mA h g⁻¹	Discharge capacity / mA h g⁻¹	Coulombic efficiency (%)
10	567	565	99.6
20	557	553	99.3
30	553	548	99.0
40	537	532	99.0
50	517	512	99.0

Reversibility increased with decreasing the current density.

The capacity of 565 mA g⁻¹ at 10 mA g⁻¹ is as high as 99.1% of the theoretical capacity of $Bi_{0.2}Sb_{0.8}$.

XRD analysis of Bi−Sb electrode during cycle

● $Bi_{0.2}Sb_{0.8}$
▼ $Na_3(Bi,Sb)$
□ Al substrate

After discharge

Bi−Sb

Discharge

After charge

$Na_3(Bi,Sb)$

Na

Before cycle

Bi−Sb

Charge

ICSD:00-001-0802(Sb)
ICSD:01-074-1160(Na₃Bi)
ICSD:03-065-3520(Na₃Sb)
ICSD:01-085-1330(Bi)

2θ(Cu-Kα) / deg. 67

Potential / V vs. Na⁺/Na

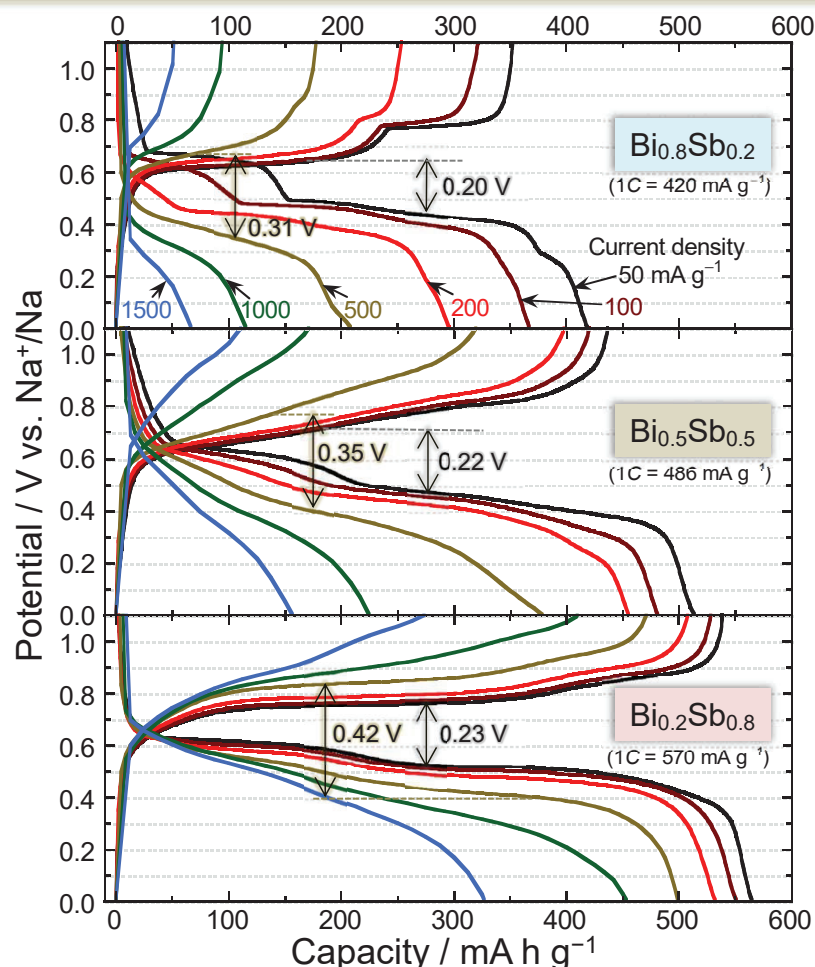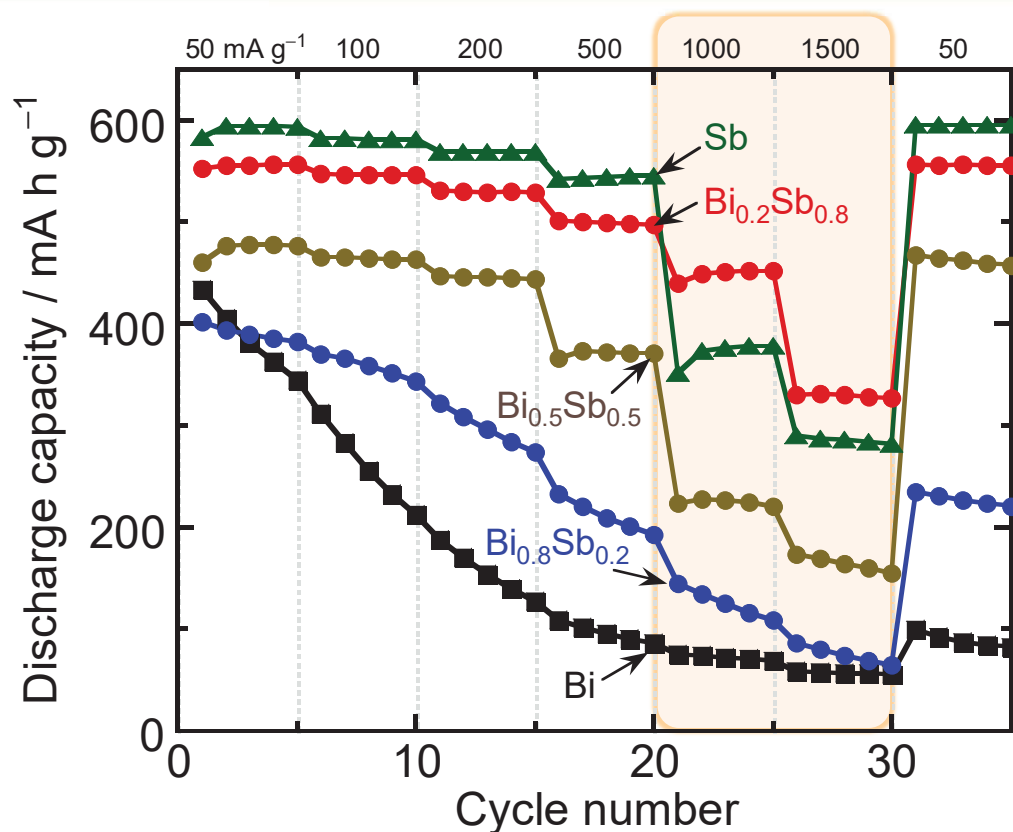Capacity / mA h g⁻¹

Charge–discharge curves of Bi–Sb at high *C*-rates

Current density / mA g^{-1}	Charge capacity / mA h g^{-1}	Discharge capacity / mA h g^{-1}	Coulombic efficiency (%)
50	419	382	91.3
100	367	343	93.5
200	295	273	92.5
500	208	193	92.5
1000	115	108	93.8
1500	67	64	95.9
50	513	476	92.8
100	481	463	96.3
200	455	444	97.5
500	378	371	98.1
1000	224	221	98.4
1500	156	155	99.0
50	565	557	98.6
100	550	546	99.2
200	532	529	99.5
500	499	497	99.7
1000	453	452	99.8
1500	327	327	99.9

Rate capability of Bi–Sb electrodes

Active material	Theoretical capacity / mA h g^{-1}
Sb	660
Bi$_{0.2}$Sb$_{0.8}$	570
Bi$_{0.5}$Sb$_{0.5}$	486
Bi$_{0.8}$Sb$_{0.2}$	420
Bi	385

Bi$_{0.2}$Sb$_{0.8}$ electrode exhibited a good rate capability at higher *C*-rates.

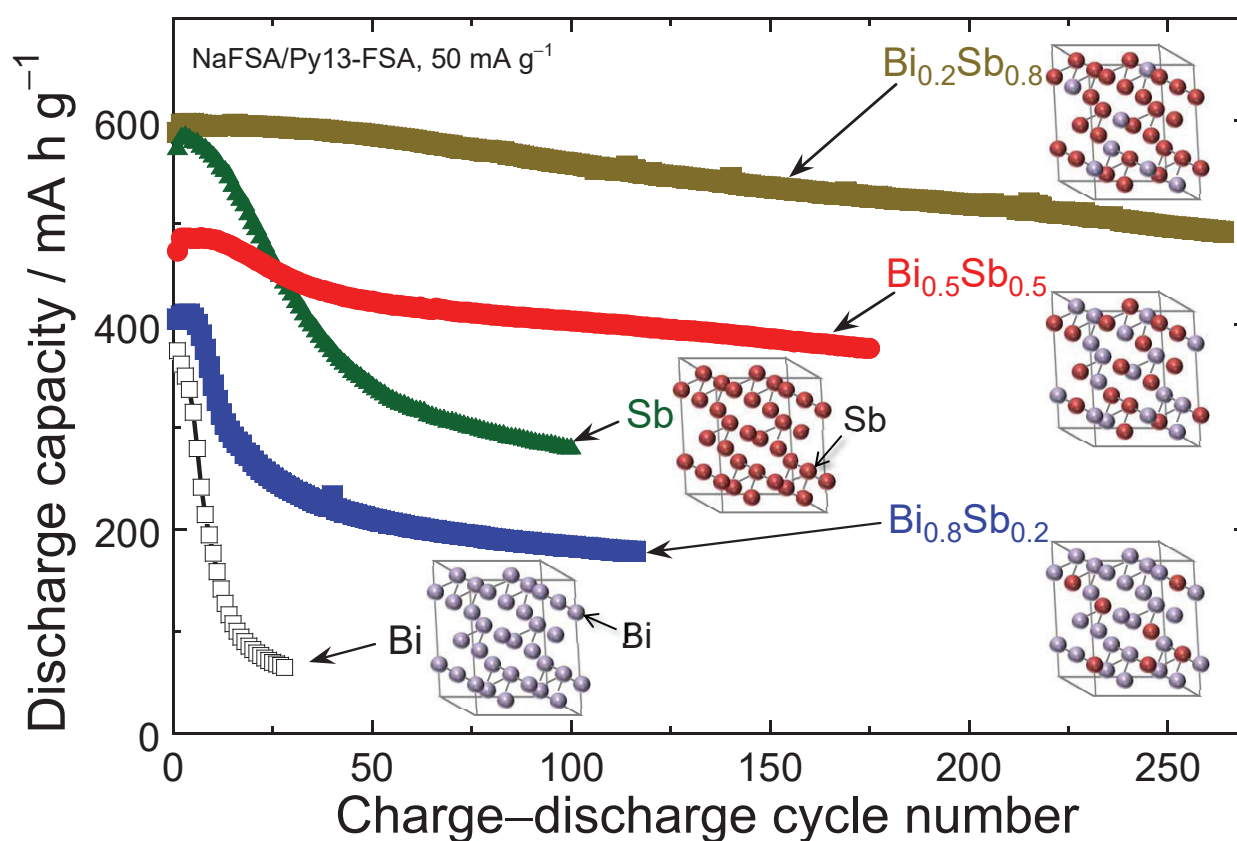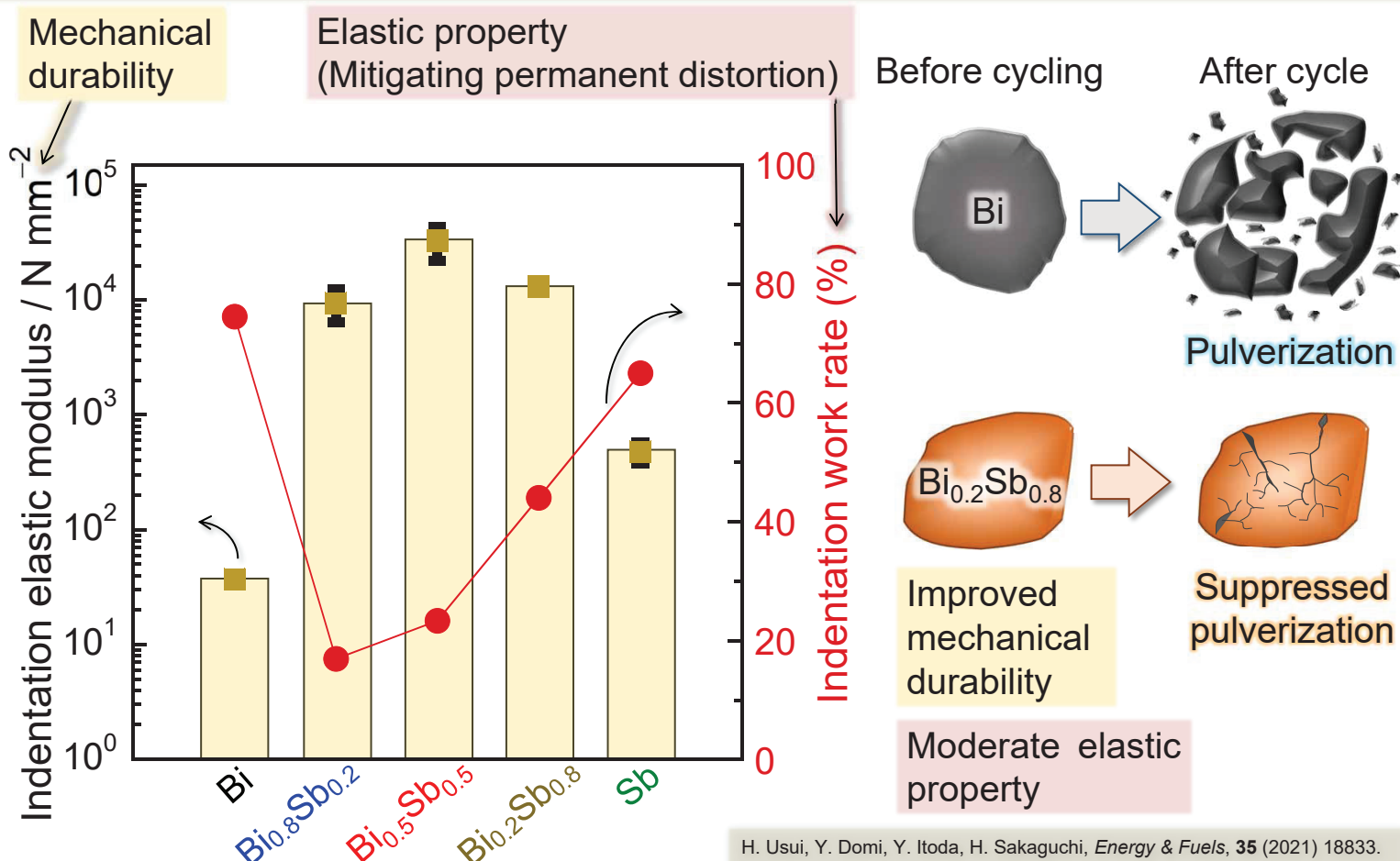# Theoretical capacity achievement rates of rate capability

Active material	Achievement rate of theoretical capacity at 1000 mA g^{-1}
Sb	57%
Bi$_{0.2}$Sb$_{0.8}$	79%
Bi$_{0.5}$Sb$_{0.5}$	47%
Bi$_{0.8}$Sb$_{0.2}$	30%
Bi	18%

Bi$_{0.2}$Sb$_{0.8}$ electrode showed the highest achievement rate of theoretical capacity.

Cycling performances of Bi−Sb electrodes

NaFSA/Py13-FSA, 50 mA g^{-1}

69

Solid solution strengthening of Bi−Sb solid solutions

Mechanical durability

Elastic property (Mitigating permanent distortion)

Before cycling → After cycle

Bi → Pulverization

$Bi_{0.2}Sb_{0.8}$ → Suppressed pulverization

Improved mechanical durability

Moderate elastic property

Surface morphology of Bi−Sb electrode after cycling

Before cycling → After 1 cycle

Bi electrode

1 µm

Bi−Sb electrode

1 µm

Before cycling → After cycle

Bi → Pulverization

$Bi_{0.2}Sb_{0.8}$ → Suppressed pulverization

Improved mechanical durability

Moderate elastic property

Solid solution strengthening could suppress electrode disintegration.

70

Summary

We evaluated Na-storage properties of Bi−Sb solid solution electrodes, and investigated the influence of galvanostatic cycling conditions on the properties.

- With increasing Sb ratio, the cycling performance improved.

- The discharge capacity and the Coulombic efficiency of the $Bi_{0.2}Sb_{0.8}$ electrode were enhanced with decreasing the charge−discharge current density from 50 to 10 mA g^{-1}.

Acknowledgements

Tottori University Faculty of Engineering building seen from the central square

Thank you for your attention.

The mascot of the University is a mandarin duck, the symbol bird of Tottori Prefecture, and represents that the University develops with the local community.

Electrochemical Polarization Part 2: Electrochemical Devices ～Capacitor~

Hiroyuki USUI,[a] Masanobu CHIKU,[b] Shin-ichi YAMAZAKI,[c] Kentaro KURATANI,[c]

Kazuhiro FUKAMI,[d] Hiroaki TSUCHIYA,[e]

[a] *Graduate School of Engineering, Tottori University, 4-101, Koyama-cho minami, Tottori, 680-8552, Japan*

[b] *Graduate School of Engineering, Osaka Metropolitan University, 1-1, Gakuen-cho, Naka-ku, Sakai, Osaka, 599-8531, Japan*
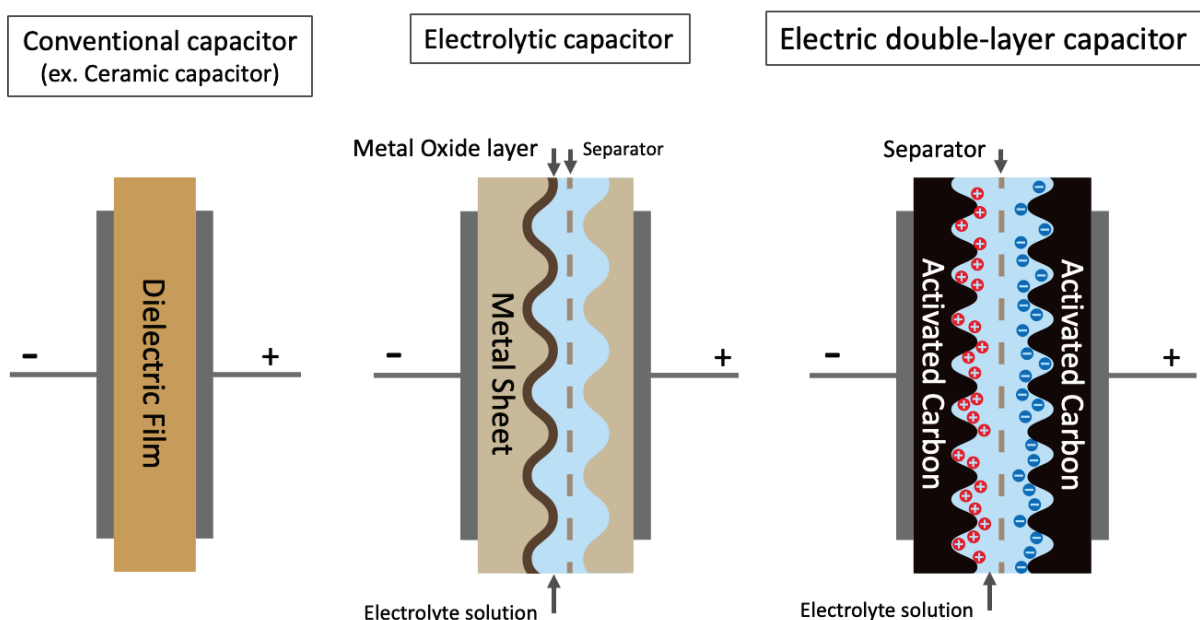
[c] *Research Institute of Electrochemical Energy, National Institute of Advanced Industrial Science and Technology (AIST), 1-8-31, Midorigaoka, Ikeda, Osaka, 563-8577, Japan*

[d] *Department of Materials Science and Engineering, Kyoto University, 36-1, Yoshida-Hommachi, Sakyo-ku, Kyoto, 606-8501, Japan*

[e] *Graduate School of Engineering, Osaka University, 2-1, Yamadaoka, Suita, Osaka, 565-0871, Japan*

What's the electrochemical capacitor ?

While conventional ceramic capacitors and electrolytic capacitors store charge through a thin film of dielectric material, electrochemical capacitors are energy storage devices that utilize the charge generated at the electrolyte-electrode interface, such as the electric double layer.
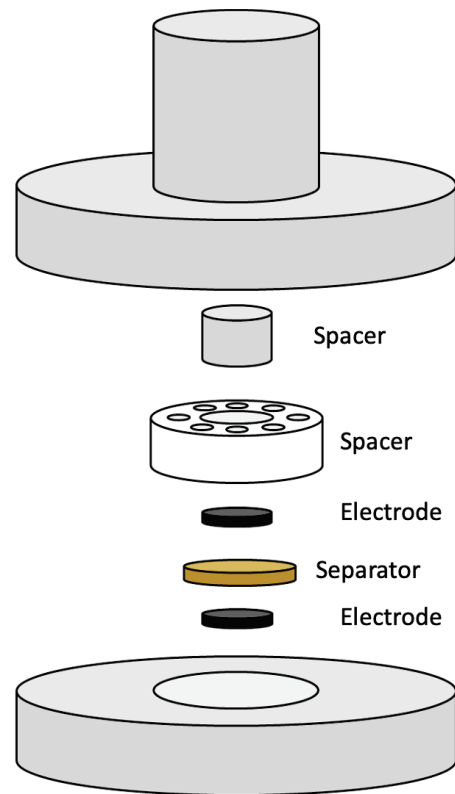

72

Method of fabricating electrochemical capacitors
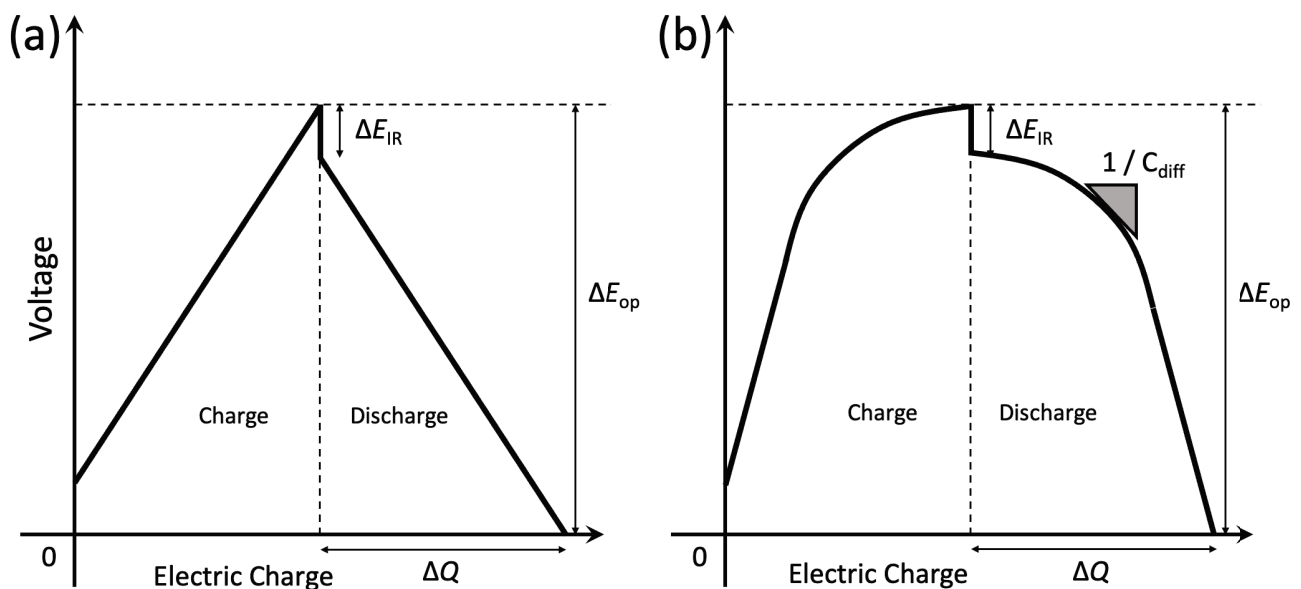
Electrodes

- Activated carbon is mainly used in electric double-layer capacitors (EDLCs).
- Various metal oxides can be used in pseudo-capacitors.
- The same material charges and discharges by a different mechanism from that of a rechargeable battery, depending on the size of the particles, for example.

Electrolyte solution

- It can be classified generally into an aqueous solution and non-aqueous solution systems.
- In aqueous solution systems, acidic and basic solutions such as sulfuric acid and potassium hydroxide are used, as well as neutral solutions.
- In non-aqueous electrolyte systems, electrolytes similar to those used in lithium-ion secondary batteries are widely used.

Spacer

Spacer

Electrode

Separator

Electrode

Charge/discharge of EDLCs

(a)

(b)

- Constant-current charge/discharge measurements are commonly used, similar to rechargeable batteries.
- However, the voltage increases in proportional to the charging time.
- Therefore, the charge-discharge curve is a triangle, unlike rechargeable batteries.
- When a redox reaction occurs due to various factors, the resulting charge-discharge curve becomes like figure (b).

The capacity of EDLCs

The capacitance of an electrochemical capacitor is defined as below;

$$C = \Delta Q / \Delta E \qquad (1)$$

If we take IR losses into account here;

$$\Delta E_{\text{IR}} = 2I \cdot R \qquad (2)$$
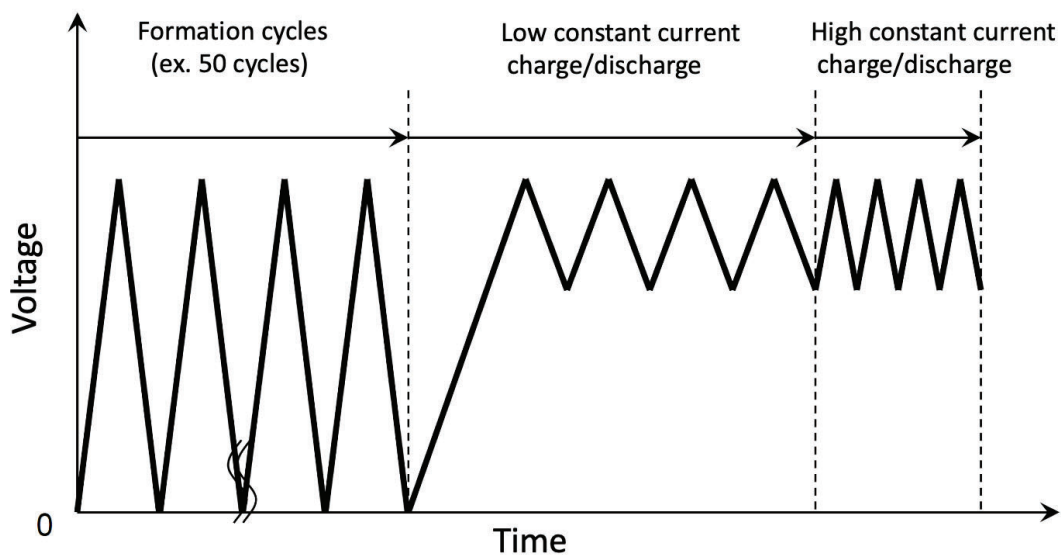
$$C_{\text{dev}} = \frac{\Delta Q}{\Delta E_{\text{op}}} \qquad (3)$$

The actual capacitance can be expressed as below;

$$C_{\text{real}} = \frac{\Delta Q}{\Delta E_{\text{op}} - \Delta E_{\text{IR}}} \qquad (4)$$

If the charge/discharge curve is strongly curved;

$$C_{\text{diff}} = \frac{\mathrm{d}Q}{\mathrm{d}E} \qquad (5)$$

Constant current charge-discharge of EDLCs

- Formation cycles of about 50 cycles before constant current charge/discharge testing are effective for consistent results.
- Measurements at varying charge/discharge current densities can provide information on the rate characteristics of the capacitor.

Notes on calculating capacitance

The capacitance of the entire cell is considered to be the positive and negative electrodes connected in series.

$$\frac{1}{C_{\mathrm{dev}}} = \frac{1}{C_{\mathrm{a}}} + \frac{1}{C_{\mathrm{c}}} \qquad (6)$$

In the case of a "symmetric cell" where the positive and negative electrodes are the same;

$$\frac{1}{C_{\mathrm{dev}}} = \frac{1}{C_{\mathrm{s}}} + \frac{1}{C_{\mathrm{s}}} = \frac{2}{C_{\mathrm{s}}} \ \Leftrightarrow \ C_{\mathrm{s}} = 2 \cdot C_{\mathrm{dev}} \qquad (7)$$

In other words, the capacity of a single electrode is twice that of the entire cell.

Notes on calculating capacitance

The relationship between the operating voltage and the amount of charge is as follows;

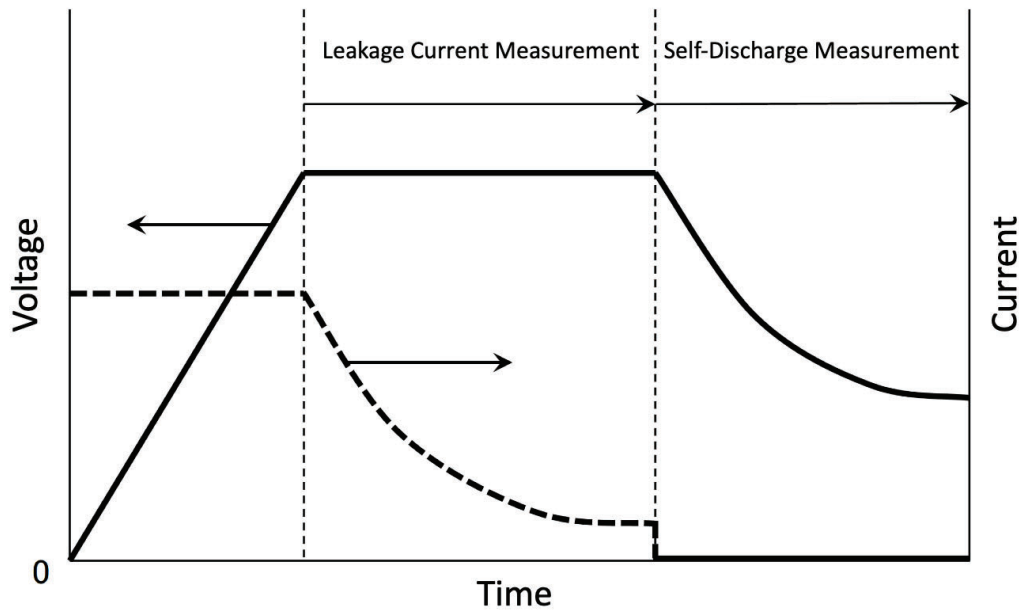$$C_{\mathrm{s}} = 2 \cdot \frac{Q}{\Delta E_{\mathrm{op}}} \qquad (8)$$

By using a constant-current charge/discharge current I

$$C_{\mathrm{s}} = 2 \cdot \frac{I \times \Delta t}{\Delta E_{\mathrm{op}}} \qquad (9)$$

From the above, the following equation is used to investigate the performance per weight, for example.
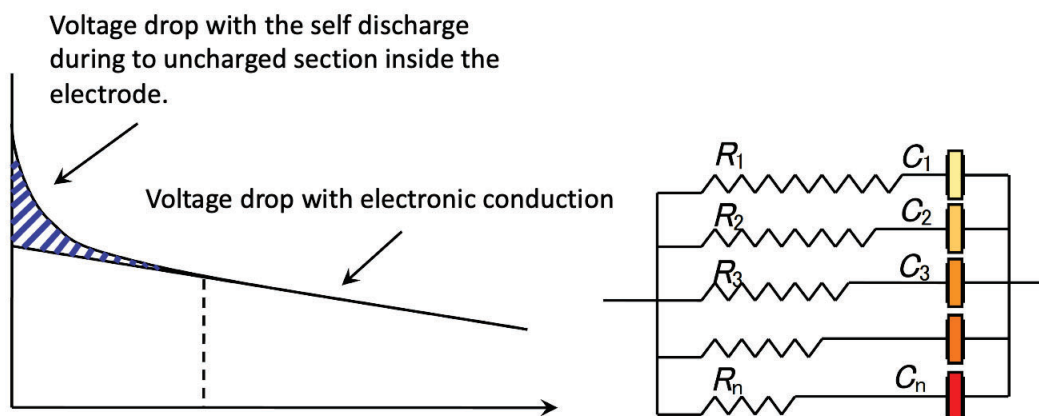
$$C_{\mathrm{sw}} = \frac{C_{\mathrm{s}}}{m_{\mathrm{s}}} = \frac{2 \cdot I \cdot \Delta t}{\Delta E_{\mathrm{op}} \cdot m_{\mathrm{s}}} \qquad (10)$$

Self-discharge and leakage current measurements

- After constant-current charging, leakage current measurement is performed with constant voltage.
- After that, self-discharge measurement is possible by opening the circuit measurement.

Self-discharge mechanism of electrochemical capacitors

- If there are uncharged sections inside the electrodes, a rapid voltage drop is seen in the early stages of the open circuit.
- If there is a discharge due to electron conduction, the cell voltage slowly decreases until it reaches zero.

Conclusions

- Capacitors store electrical energy through electrochemical reactions similar to secondary batteries, but the charging and discharging mechanisms and time scales are significantly different.

- In constant-current charge-discharge tests, a plateau voltage like that of secondary batteries is not observed, and the voltage is proportional to time and triangular in shape.

- Leakage current and self-discharge measurements can be used to estimate electrode problems.

Electrochemical Polarization Part 2: Electrochemical Devices ~Fuel cell~

Hiroyuki USUI,[a] Masanobu CHIKU,[b] Shin-ichi YAMAZAKI,[c] Kentaro KURATANI,[c]

Kazuhiro FUKAMI,[d] Hiroaki TSUCHIYA,[e]

[a] *Graduate School of Engineering, Tottori University, 4-101, Koyama-cho minami, Tottori, 680-8552, Japan*

[b] *Graduate School of Engineering, Osaka Metropolitan University, 1-1, Gakuen-cho, Naka-ku, Sakai, Osaka, 599-8531, Japan*

[c] *Research Institute of Electrochemical Energy, National Institute of Advanced Industrial Science and Technology (AIST), 1-8-31, Midorigaoka, Ikeda, Osaka, 563-8577, Japan*

[d] *Department of Materials Science and Engineering, Kyoto University, 36-1, Yoshida-Hommachi, Sakyo-ku, Kyoto, 606-8501, Japan*

[e] *Graduate School of Engineering, Osaka University, 2-1, Yamadaoka, Suita, Osaka, 565-0871, Japan*

A polymer electrolyte fuel cell (PEFC)

➤ A present PEFC is composed of Pt/C catalysts and perfluorosulfonic acid membrane electrolyte.

➤ A PEFC is operated under steady-state conditions for practical use.

➡ The steady-state polarization is frequently analyzed to assess performance.
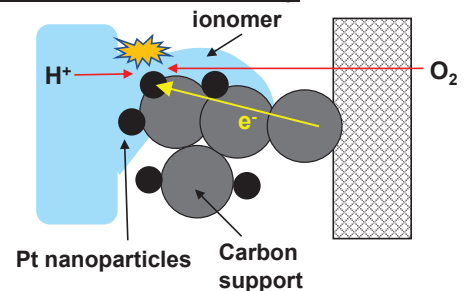
A schematic description of PEFC

- anode separator (current collector)
- anode GDL/MPL
- anode catalyst layer
- electrolyte membrane
- cathode catalyst layer
- cathode GDL/MPL
- cathode separator (current collector)

Membrane electrode assembly (MEA)

GDL: gas diffusion layer

MPL: microporous layer

Triple-phase boundary

Page 1

78

Evaluation of MEA performance

Catalyst → Preparation of catalyst ink → Preparation of catalyst layer → Preparation of MEA

anode separator   MEA   cathode separator

H_2 ⟶ ⟵ O_2

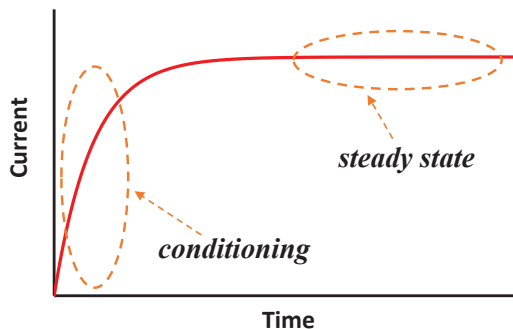anode GDL/MPL   cathode GDL/MPL

"Conditioning" before the data acquisition

A MEA with a Pt cathode catalyst does not reach a steady state immediately after the start of current loading; the potential increases gradually with time.

➡ "Conditioning" (or "break-in") is needed

Constant-potential operation, constant-current operation, or repeated *IV* measurements

◆ **Constant-potential conditioning**

steady state

conditioning

Current vs. Time

➢ H_2O is generated during conditioning.

➢ After the current (or potential) reaches steady state, polarization is measured.
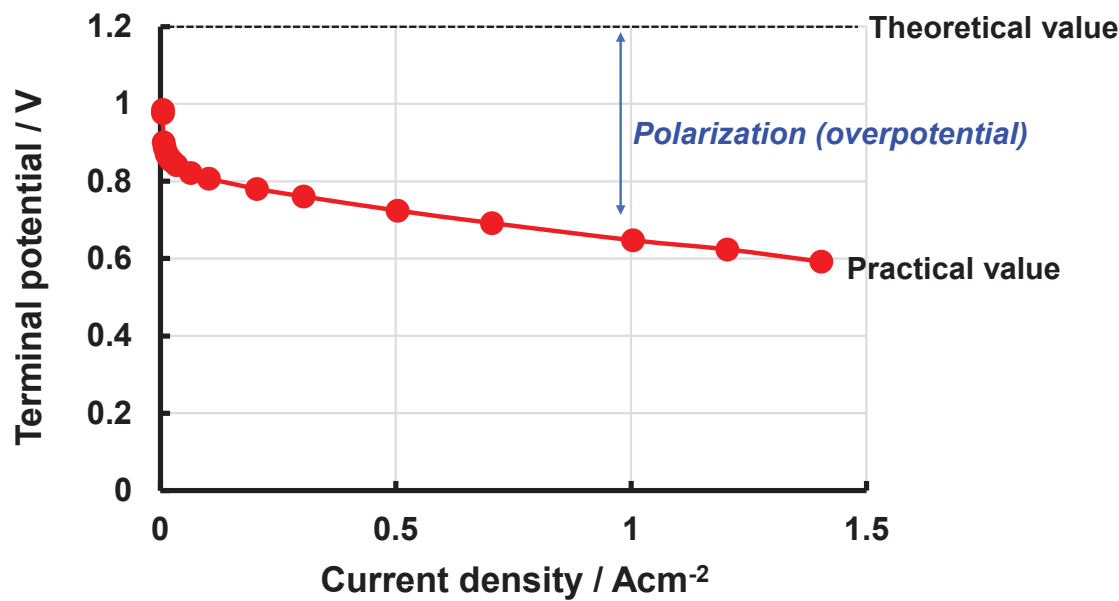
◆ **Effects of conditioning**

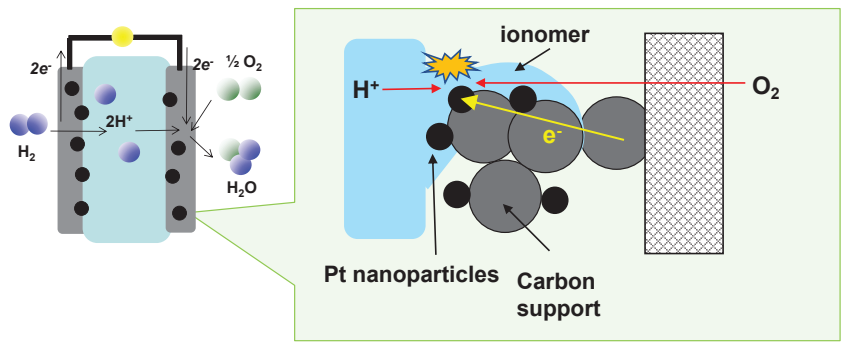(1) Wash-out of impurities from the Pt surface

H_2O ⟶

(2) Hydration of the electrolyte membrane

H_2O ⟶

T. D. Gierke et al., Perfluorinated Ionomer Membranes.,Chapter 13, 283-307 (1982) Reprinted with permission. Copyright (1982) American Chemical Society.

Polarization curve (*IV* curve)

Breakdown of overpotentials

(1) Resistance overpotentials

→ **The resistance of H^+ transportation in the electrolyte**

Electrical resistance and contact resistance of components

(2) Activation overpotentials

→ **The electrode kinetics of cathode**

(H₂ oxidation proceeds rapidly on the Pt anode, and the anode overpotential can be neglected.)

(3) Diffusion overpotentials

→ **O_2 diffusion**

Separation of the overpotentials

How can each overpotential be assessed from *IV* curve?

(1) Resistance overpotentials

    IR (Current × resistance)

      ↳ AC impedance spectroscopy

    IR-free potential = observed potential − IR

Calculated *IR*-free *IV* curve from the Tafel slope

Activation overpotential

"diffusion" overpotential

Measured *IR*-free *IV* curve

IR-free potential (axis)

Current density

(2) Activation overpotentials

    It obeys Tafel law.

      ↳ Log |*I*| is linear to *E*

(3) "Diffusion" overpotentials

    The deviation of observed potential from the potential calculated from the Tafel slope

---

Activation overpotentials –Tafel slope (1) –

"Simple" Tafel law

$$I = I_0 \exp(-\alpha n F \eta / RT)$$

    α : transfer coefficient

    n : number of electrons transferred in rate-determining step

    F : Faraday constant (C mol^{-1})

    η : overpotential (V)

    R : gas constant (J mol^{-1}K^{-1})

    T : Temperature (K)

Tafel plot

Tafel slope

$$-2.303 \, RT/\alpha n F$$

E

log |*I*|

Does Tafel slope directly indicate the *n* value?

➡ **No, it does not necessarily mean the *n* value**

Activation overpotentials –Tafel slope (2) –

The Tafel slope does not necessarily mean the *n* value

- ➤ Case 1: when pre- and post-reaction affects the rate-determining step
- ➤ Case 2: the number of active sites depends on the potential

Case 2

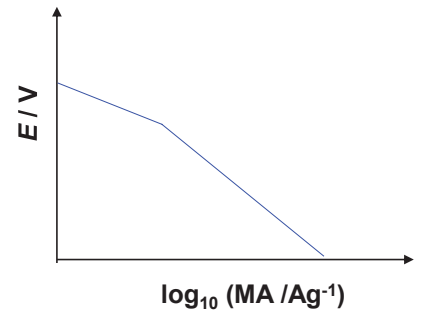Pt surface is coverage by O-derived species (e.g. Pt-OH) at high potentials.

➡ **The real active surface area of Pt depends on the potential.**

$$i = i_0 \left(\frac{P_{O2}}{P_{O2,ref}} \right)^{\gamma} (1-\theta) \exp\left(\frac{-\alpha F \eta}{RT} \right) \exp\left(\frac{-\omega \theta}{RT} \right)$$

$$\frac{1}{\text{Tafel slope}} = -\frac{\alpha F}{2.303 RT} - \frac{1}{2.303} \left(\frac{1}{1-\theta} + \frac{\omega}{RT} \right) \left(\frac{\partial \theta}{\partial E_{IR-free}} \right)$$

θ : the oxide coverage ω : the energy parameter for the Temkin isotherm

N. P. Subramanian, et al., *J. Electrochem. Soc.*, **159**, B531 (2012)

(graph: E / V vs log₁₀ (MA /Ag⁻¹))

"Diffusion" overpotentials

Observed potential departs from the calculated Tafel curve at high currents

Possible reasons

- ➤ The potential was dropped by the limitation of O_2 diffusion
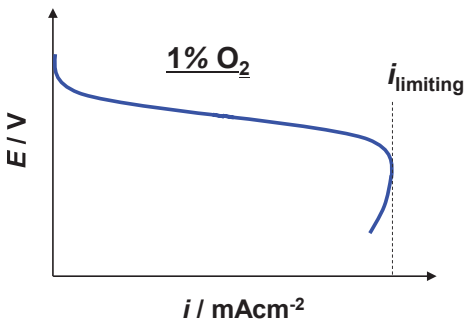- ➤ Change of Tafel slope (reaction proceeds another reaction mechanism

Schematic description of O_2 transportation in PEFC

Breakdown of O$_2$ transportation resistance (1)

$R_{total} = (4FP_{O2})/(RT\,i_L)$

R_{total} can be determined from the limiting current under diluted O$_2$ conditions.

R_{total} : total resistance (s cm^{-1})

F : Faraday constant (A s mol^{-1})

R : gas constant (J mol^{-1}K^{-1})

i : limiting current density (Acm^{-2})

P_{O2} : MPa

T : Temperature (K)

Three resistances

(1) Fickian diffusion of O$_2$ in gas channel and macropores in gas diffusion layer (R_F)

➡ Originates from the collision of O$_2$ with gaseous molecules

(2) Knudsen diffusion of O$_2$ in micropores in catalyst layer and microporous layer (R_{Kn})

➡ Originates from the collision of O$_2$ with the wall of micropores

(3) O$_2$ diffusion near the Pt surface (local O$_2$ resistance, R_L)

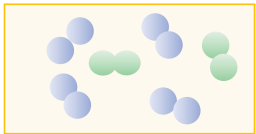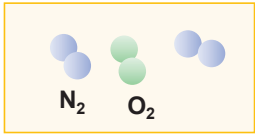➡ Originates from the diffusion in ionomer near Pt nanoparticles

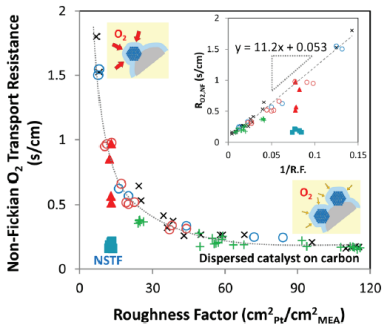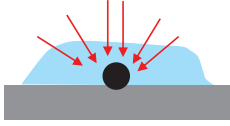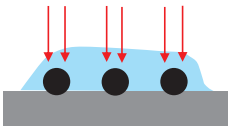$R_{total} = R_F + R_{Kn} + R_L$ H. Yamada, et al., *J. Electrochem. Soc.*, **167**, 084508 (2020)

Breakdown of O$_2$ transportation resistance (2)

Near Pt (R_L)   Micro pores (R_{Kn})   Macro pores (R_F)   GDL (R_F)

H$^+$ e$^-$ O$_2$

(1) R_F is proportional to pressure.

N$_2$ O$_2$

(3) $1/R_L$ is proportional to surface area of Pt.

A. Kongkanand, et al., *J. Phys. Chem. Lett.*, **7**, 1127 (2016) Reprinted with permission. Copyright (2016) American Chemical Society.

R_{total} / (s/m)

R_{other}

Pressure (MPa)

Non-Fickian O$_2$ Transport Resistance (s/cm)

$y = 11.2x + 0.053$

$R_{O2,NF}$ (s/cm)

1/R.F.

NSTF   Dispersed catalyst on carbon

Roughness Factor (cm$^2_{Pt}$/cm$^2_{MEA}$)

H. Yamada, et al., *J. Electrochem. Soc.*, **167**, 084508 (2020)

T. A. Greszler, et al., *J. Electrochem. Soc.*, **159**, F831 (2012)

Summary (polarization of MEA)

Analysis of Steady-state polarization (overpotentials)

> "Conditioning" is needed to acquire steady-state parameters.

> Polarization of MEA is divided into three overpotentials: (1) resistance overpotential, (2) activation overpotentials, (3) "diffusion" overpotential

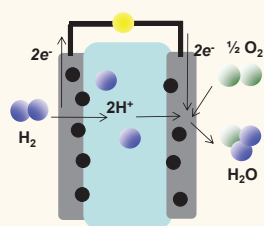> (2) activation overpotentials obeys <u>expanded Tafel lows</u>.

$$\downarrow$$

The site blocking effect of Pt-OH is taken into consideration.

> (3) "Diffusion" overpotentials can be divided into three resistances: R_F (in GDL), R_{Kn} (in microporous layer), R_L (near Pt nanoparticles)

➡ Each overpotential can be separated from the dependence of total resistance on pressure and Pt surface area.

Rotating disk electrode (RDE) method for rapid screening of Pt catalysts
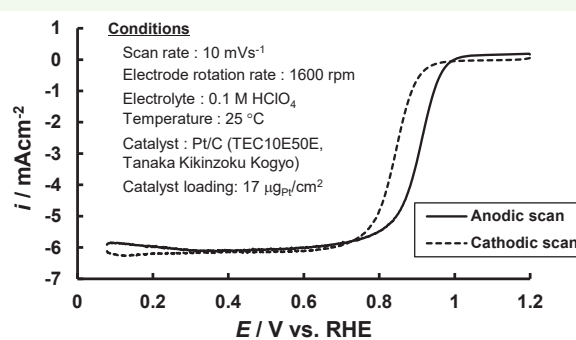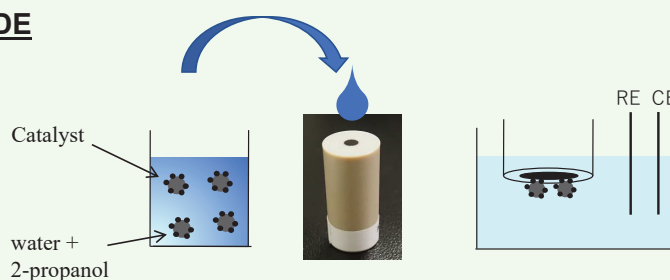
MEA

2e⁻   2e⁻   ½ O₂

H₂   2H⁺   H₂O

> Time consuming

> Depends on the elaboration

> All information is included

Not suitable for rapid screening and the assessment of intrinsic activity of catalysts

RDE

Catalyst

water + 2-propanol

RE CE

Conditions
Scan rate : 10 mVs⁻¹
Electrode rotation rate : 1600 rpm
Electrolyte : 0.1 M HClO₄
Temperature : 25 °C
Catalyst : Pt/C (TEC10E50E, Tanaka Kikinzoku Kogyo)
Catalyst loading: 17 µg$_{Pt}$/cm²

— Anodic scan
---- Cathodic scan

i / mAcm⁻² vs. E / V vs. RHE

Diffusion layer under static and electrode-rotation conditions
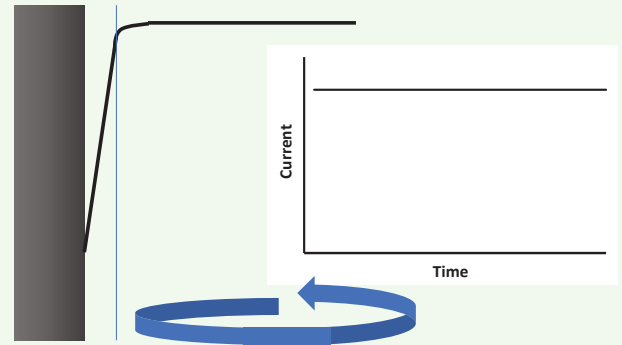
◆ **Static**

◆ **Rotation of electrode**

➢ **The length of diffusion layer increases with time.**

➡ **The current decreased with time.**

$$I = nFAC_B(D/\pi t)^{1/2}$$

D : diffusion coefficient (cm^{2}s^{-1})

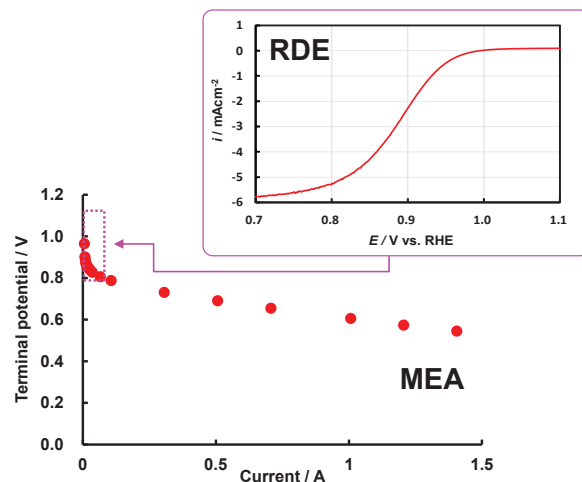➢ **The length of diffusion layer is constant.**

➡ **The steady-state current**

Pros and Cons of an RDE method

Merits of RDE method

➢ **Slight amount of catalyst**

➢ **Shorter time**

➢ **The activity can be evaluated under well-defined conditions.**

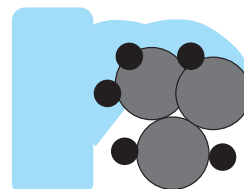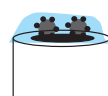➢ **The results does not depend on the elaboration.**

Demerits of RDE method

➢ **Information at high currents is missing.**

➢ **The effect of Nafion is difficult to analyze.**

➢ **The effect of humidity cannot be evaluated.**
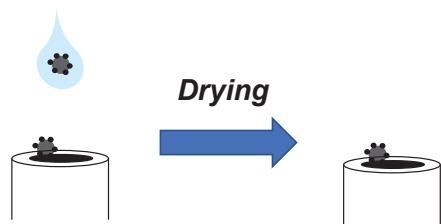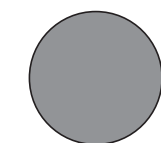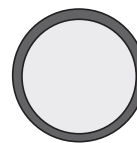
➢ **Evaluation at a high temperature is difficult**

RDE

MEA

Immobilization of catalyst on RDE

Drying

> Homogenous dispersion of catalyst is important for the accurate evaluation.

The quality of modified electrode depends on the immobilization method.

Homogeneous dispersion

"Coffee ring" effect

◆ **Parameters**

> **Solvent of suspension**

> **Coating method**

> **Drying rate**

> **Atmosphere when drying**

> **Nafion coating**

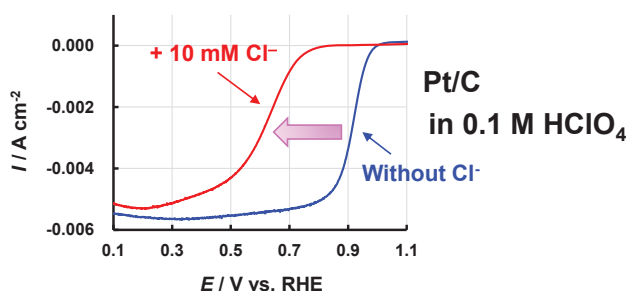K. Ke, et al., *Electrochim. Acta*, **72**, 120 (2012)

U. A. Paulus et al., *J. Electroanal. Chem.,* **495,** 134 (2001).

N. Aoki, et al., *Electrochim. Acta*, **244**, 146 (2017)

A reference electrode and electrolyte for the evaluation of Pt catalysts

◆ **Reference electrode**

> **Pt catalysts are vulnerable to adsorption of electrolyte component and impurity.**

+ 10 mM Cl^-

I / A cm^{-2}

Pt/C in 0.1 M $HClO_4$

Without Cl^-

E / V vs. RHE

The contamination of Cl^- must be avoided.

An Ag|AgCl|KCl reference electrode

→ Release of Cl^-

A reversible hydrogen electrode (RHE)

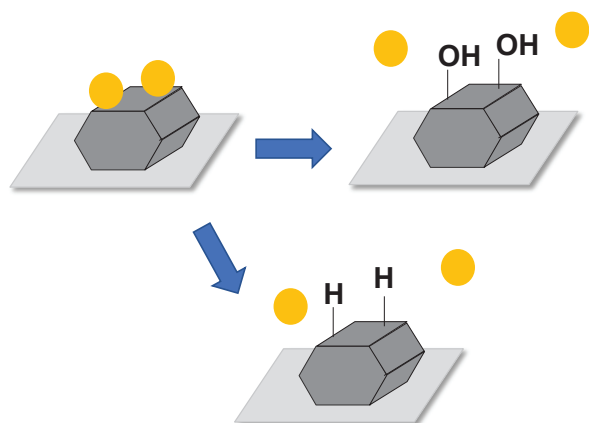→ no contamination

◆ **Electrolyte & Cell**

> **The specific adsorption of ClO_4^- is weaker than those of SO_4^{2-}, PO_4^{3-}, and Cl^-**

➡ **A diluted $HClO_4$ solution (0.1 M) is used as electrolyte solution.**

> **The highly purified ClO_4^- and water should be used.**
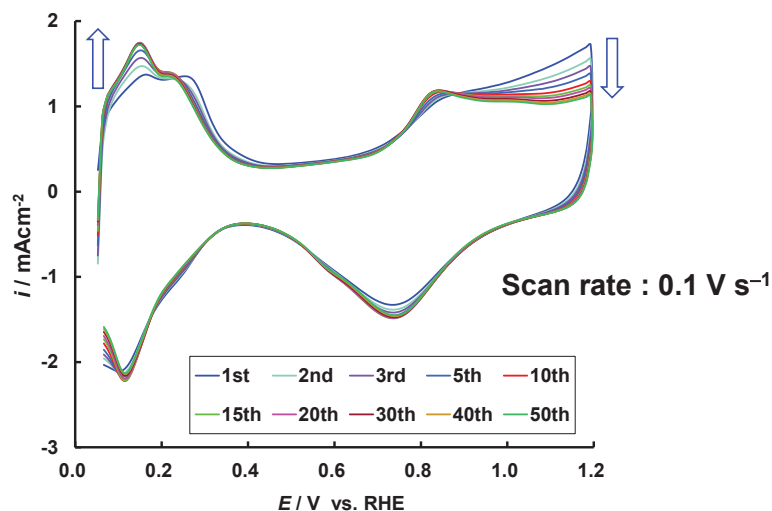
> **The cell should be sometimes washed with strong acid.**

Conditioning of RDE

The surface of Pt is covered with poisoning species. ➡️ **Repeated pre-scans of cyclic voltammograms**
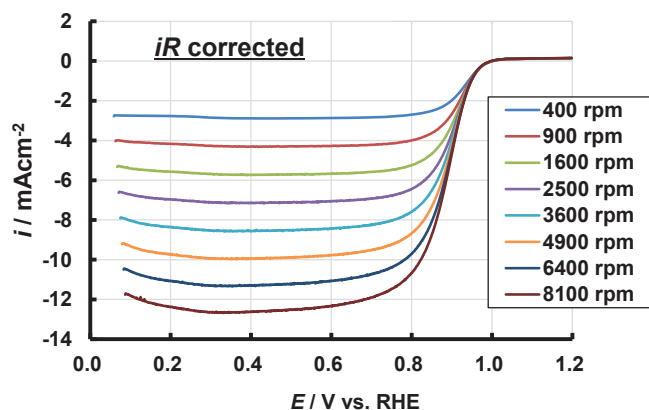

Scan rate : 0.1 V s^{-1}

Legend: 1st, 2nd, 3rd, 5th, 10th, 15th, 20th, 30th, 40th, 50th

Cleaning of Pt surface

➡️ **Pt surface reaches steady state.**

Typical LSVs and calculation of MA

iR corrected

Legend: 400 rpm, 900 rpm, 1600 rpm, 2500 rpm, 3600 rpm, 4900 rpm, 6400 rpm, 8100 rpm

Conditions
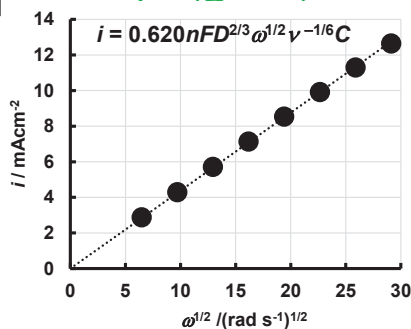
Scan rate : 10 mVs^{-1}

Electrode rotation rate : 1600 rpm

Electrolyte : 0.1 M HClO$_4$

Temperature : 25 °C

Catalyst : Pt/C (TEC10E50E, Tanaka Kikinzoku Kogyo)
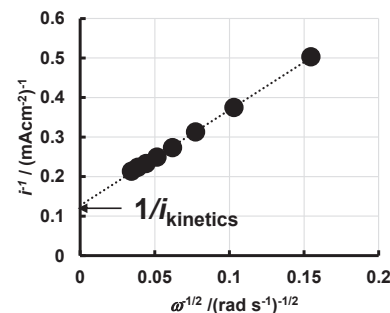
Catalyst loading: 17 μg$_{Pt}$/cm^2

$R_{total} = R_{kinetics} + R_{diffusion}$

$1 / I = 1 / I_{kinetics} + 1 / I_{limiting}$

$\longrightarrow I_{kinetics} = I_{limiting} \times I / (I_{limiting} - I)$

Mass activity = $I_{kinetics}$ / (Pt loading)

◆ **Levich plot (@0.38 V)**

$i = 0.620nFD^{2/3}\omega^{1/2}\nu^{-1/6}C$

◆ **Koutecky-Levich plot (@0.9 V)**

$1/i_{kinetics}$

D : diffusion coefficient (cm^{2}s^{-1})

ω : rotation rate

ν : kinematic viscosity (cm^{2}s^{-1})

Direction of scans – effect of Pt oxide formation/reduction –

$$i \text{ / mAcm}^{-2}$$

— Anodic scan
---- Cathodic scan

E / V vs. RHE

H_2O_{aq} (C)

$H_2O_{aq} \leftrightarrow OH_{ad} + H^+_{aq} + e^-$

OH_{ad}

$2OH_{ad} \rightarrow O_{ad} + H_2O_{aq}$

$OH_{ad} \leftarrow O_{ad} + H^+_{aq} + e^-$

O_{ad}

R. Jinnouchi, et al., *J. Chem. Phys.*, **142**, 184709 (2015)
Reprinted with permission. Copyright (2015) AIP Publishing

The catalytic activity depends on the direction of scan (hysteresis).

➡ **Effect of Pt oxide formation**

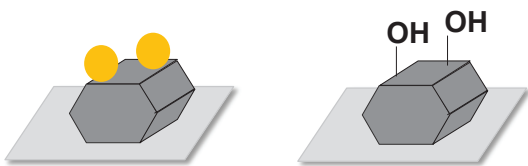# The effect of scan rate and electrode rotation rate

◆ **Scan rate**

High scan rate

➡ **Steady-state conditions are not met.**

Low scan rate ➡ **Lower activity**

➤ **Adsorption of Impurity**
➤ **Pt oxide formation**

OH OH

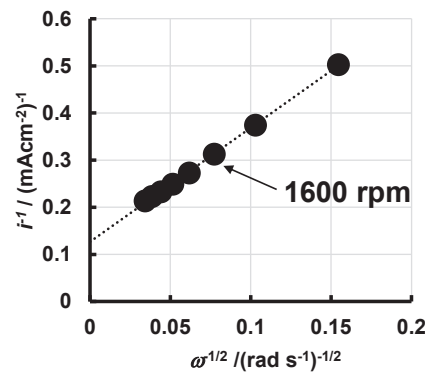K. Shinozaki, et al., *J. Electrochem. Soc.*, **162**, F1144 (2015)

◆ **Rotation rate**

Lower rotation rate

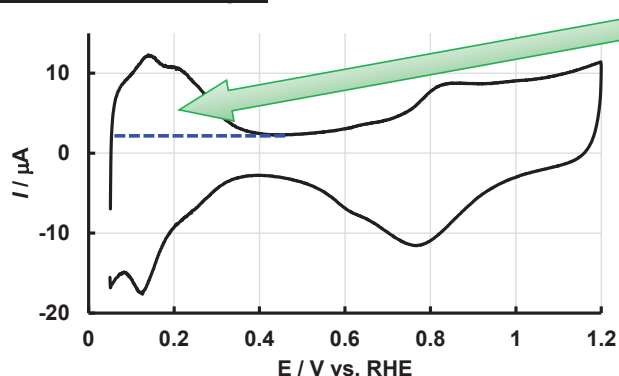➡ **Highly active catalyst cannot be examined.**

Higher rotation rate

➡ **Deviation from K-L plot**

$$i^{-1} \text{ / (mAcm}^{-2})^{-1}$$

1600 rpm

$\omega^{1/2}$ /(rad s^{-1})$^{-1/2}$

Electrochemically active surface area (ECSA)

CVs of a Pt catalyst

The formation of Pt-H

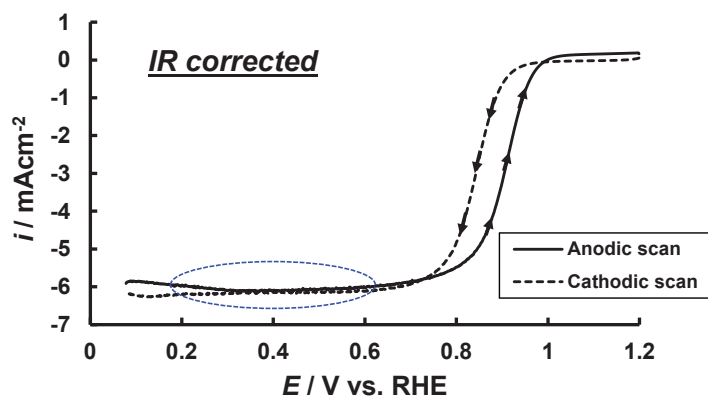**Electrochemically active surface area (ECSA) can be determined from the peak area of Pt-H**

Conversion coefficient : 0.21 mC / cm^2_{Pt}

Conditions

Scan rate : 10 mVs^{-1} Catalyst loading: 17 $\mu g_{Pt}/cm^2$

Electrolyte : Ar-saturated 0.1 M HClO$_4$

Temperature : 25 °C

Catalyst : Pt/C (**TEC10E50E**, Pt 46.5wt%, Tanaka Kikinzoku Kogyo)
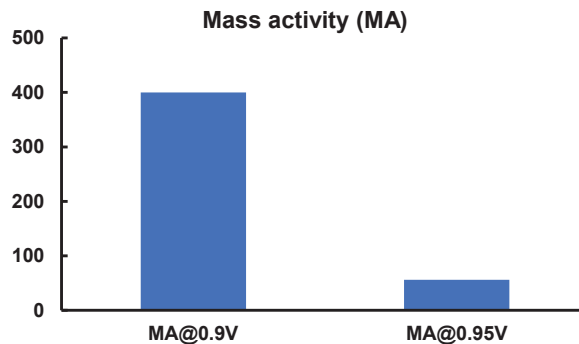

Typical results

IR corrected

Conditions

Scan rate : 10 mVs^{-1} Catalyst loading: 17 $\mu g_{Pt}/cm^2$

Electrode rotation rate : 1600 rpm

Electrolyte : O$_2$-saturated 0.1 M HClO$_4$

Temperature : 25 °C

Catalyst : Pt/C (**TEC10E50E**, Pt 46.5wt%, Tanaka Kikinzoku Kogyo)

$R_{total} = R_{kinetics} + R_{diffusion}$

$1 / I = 1 / I_{kinetics} + 1 / I_{limiting}$

$\longrightarrow I_{kinetics} = I_{limiting} \times I / (I_{limiting} - I)$

Mass activity = $I_{kinetics}$ / (Pt loading)

Mass activity (MA)

What's wrong?

Phenomena

> The current does not reach a (theoretical) limiting current.

> The shape of CV is different from that of Pt.

Diagnostics

> Homogeneous dispersion of catalyst powder on the surface of an electrode

> Removal of impurity

> *IR* correction

> Direction *of* scans

Summary of RDE measurements

> A RDE method is a convenient method for the assessment of the activity of Pt catalysts.

> A steady-state conditions are attained by rotating electrode.

> For the accurate evaluation, immobilization of catalyst on an electrode, reference electrode, purity of electrolyte solution, and cleaning of the cell are important.

> Direction of scans affects the oxygen reduction activity of Pt catalysts because Pt-OH formation involves hysteresis.

> A scan rate and rotation rate have to be set appropriately.